Topoisomerase I-mediated cleavage at unrepaired ribonucleotides generates DNA double-strand breaks

Appendix

Shar-yin N. Huang [1,*], Jessica S. Williams [2,*], Mercedes E. Arana [2], Thomas A. Kunkel [2] and Yves Pommier [1,#]

[1] Developmental Therapeutics Branch and Laboratory of Molecular Pharmacology, Center for Cancer Research, National Cancer Institute, NIH, Bethesda, MD 20892.
[2] Genome Integrity and Structural Biology Laboratory, National Institute of Environmental Health Sciences, NIH, Research Triangle Park, NC 27709.
[*] These authors contributed equally to this work.
[#] Corresponding author: Email: pommier@nih.gov

Table of Contents

Appendix Table S1
Appendix Table S2
Appendix Table S3
Appendix Figure S1
Appendix Figure S2
Appendix Figure S3
Appendix Figure S4
Appendix References

Appendix Table S1 - Specific mutation rates ($x10^{-8}$) for individual mutation classes of *URA3* reporter gene in orientation 2

Strain	Overall Rate	Δ 2–5 bp	BPS	±1 frameshifts
WT	2.1	0.018	1.2	0.18
rnh201Δ	5.1	1.8	1.7	0.26
rnh201Δ rad52Δ	45	0.97	30	8.1

BPS; base pair substitutions. Specific mutation rates were calculated as the proportion of each type of event among the total mutants sequenced, multiplied by the mutation rate for each strain (using the data shown in Fig EV2). Sequencing data is from (Nick McElhinny et al., 2010) for the *WT* strain and from (Clark et al., 2011) for the *rnh201Δ* strain. Consistent with previous results (Clark et al., 2011, Kim et al., 2011), loss of *RNH201* caused a small (2-3 fold) increase in overall mutation rate. Deletion of *RAD52* caused an approximately 30-fold increase in the spontaneous mutation rate for both reporters, in agreement with previous studies (Kunz et al., 1989, Kunz et al., 1998). In these studies, the elevated mutation rate in *rad52Δ* cells has been attributed to translesion synthesis (TLS) by Pol ζ (Rev3 in yeast). Inactivation of *RAD52* blocks the repair of spontaneous DNA lesions through the error-free HR pathway and channels them into the TLS repair pathway instead, leading to a high rate of Rev3-dependent single base substitutions (Endo et al., 2007, Huang et al., 2002, Kunz et al., 1998, Roche et al., 1995). The high overall mutation rate of a *rad52Δ* mutant was not significantly changed following additional loss of *RNH201*, or *TOP1*, or both. This suggests that the generation and/or repair of the majority the spontaneous DNA damage that arises in *rad52Δ* cells are independent of unrepaired ribonucleotides and/or Top1 activity.

Appendix Table S2 - *S. cerevisiae* strains

Name	Strain	Relevant Genotype	Source
WT	YJW588	*wt* + Rad52-YFP*:LEU2*	This study
rnh201Δ	YJW590	*rnh201::hphMX4* + Rad52-YFP*:LEU2*	This study
top1Δ	YJW598	*top1::natMX4* + Rad52-YFP*:LEU2*	This study
top1Δ rnh201Δ	YJW596	*top1::natMX4 rnh201::hphMX4* + Rad52-YFP*:LEU2*	This study
rnh201-RED	YJW836	*rnh201-P45D-Y219A:HphMX6* + Rad52-YFP*:LEU2*	This study
rnh201-RED top1Δ	YJW839	*rnh201-P45D-Y219A:HphMX6 top1::natMX4* + Rad52-YFP*:LEU2*	This study
rnh1Δ		*rnh1::natMX4* + Rad52-YFP*:LEU2*	This study
rnh201-RED rnh1Δ	YJW827	*rnh201-P45D-Y219A:HphMX6 rnh1::natMX4* + Rad52-YFP*:LEU2*	This study
WT	SNM8	*agp1::URA3-OR1*	(Nick McElhinny et al., 2010)
WT	SNM18	*agp1::URA3-OR2*	(Nick McElhinny et al., 2010)
rnh201Δ	SNM106	*rnh201::hphMX4 agp1::URA3-OR1*	(Nick McElhinny et al., 2010)
rnh201Δ	SNM114	*rnh201::hphMX4 agp1::URA3-OR2*	(Nick McElhinny et al., 2010)
pol2-M644G	SNM70	*pol2-M644G*	(Nick McElhinny et al., 2010)
pol2-M644G rnh201Δ	SNM120	*pol2-M644G rnh201::hphMX4*	(Nick McElhinny et al., 2010)

rnh201Δ top1Δ	YJW77	*rnh201::hphMX4 top1::natMX4 agp1::URA3-OR2*	(Kim et al., 2011)
top1Δ	YJW81	*top1::natMX4 agp1::URA3-OR2*	(Williams et al., 2013)
pol2-M644G top1Δ	YJW85	*pol2-M644G top1::natMX4*	(Williams et al., 2013)
pol2-M644G rnh201Δ top1Δ	YJW91	*pol2-M644G rnh201::hphMX4 top1::natMX4*	(Williams et al., 2013)
rad51Δ	YJW102	*rad51::natMX4*	This study
pol2-M644G rnh201Δ rad51Δ	YJW106	*pol2-M644G rnh201::hphMX4 rad51::natMX4*	This study
pol2-M644G rad51Δ	YJW111	*pol2-M644G rad51::natMX4*	This study
rnh201Δ rad51Δ	YJW117	*rnh201::hphMX4 rad51::natMX4*	This study
rad51Δ top1Δ	YJW244	*rad51::natMX4 top1::LEU2*	This study
pol2-M644G rnh201Δ rad51Δ top1Δ	YJW247	*pol2-M644G rnh201::hphMX4 rad51::natMX4 top1::LEU2*	This study
pol2-M644G rad51Δ top1Δ	YJW249	*pol2-M644G rad51::natMX4 top1::LEU2*	This study
rnh201Δ rad51Δ top1Δ	YJW252	*rnh201::hphMX4 rad51::natMX4 top1::LEU2*	This study
pol2-M644G rnh201-RED	YJW409	*pol2-M644G rnh201-P45D-Y219A:HphMX6*	This study

top1Δ	YJW636	*top1::LEU2 agp1::URA3-OR2*	This study
rnh201Δ top1Δ	YJW638	*rnh201::hphMX4 top1::LEU2 agp1::URA3-OR2*	This study
pol2-M644G top1Δ rnh201-RED	YJW708	*pol2-M644G top1::LEU2 rnh201-P45D-Y219A:HphMX6*	This study
pol2-M644G rad51Δ rnh201-RED	YJW712	*pol2-M644G rad51::natMX4 rnh201-P45D-Y219A:HphMX6*	This study
pol2-M644G rad51Δ rnh201-RED	YJW726	*pol2-M644G rad51::natMX4 rnh201-P45D-Y219A:hphMX6 top1::LEU2*	This study
rad52Δ	MEA17	*rad52::natMX4 agp1::URA3-OR1*	This study
rad52Δ	YJW633	*rad52::natMX4 agp1::URA3-OR2*	This study
top1Δ rad52Δ	YJW664	*top1::LEU2 rad52::natMX4 agp1::URA3-OR2*	This study
rnh201Δ rad52Δ	MEA49	*rnh201::hphMX4 rad52::natMX4 agp1::URA3-OR1*	This study
rnh201Δ rad52Δ	YJW322	*rnh201::hphMX4 rad52::natMX4 agp1::URA3-OR2*	This study
rnh201Δ rad52Δ top1Δ	YJW667	*rnh201::hphMX4 rad52::natMX4 agp1::URA3-OR2*	This study
top1-5FLAG	YJW705	*top1-5FLAG:natMX6*	This study
top1-5FLAG rnh201Δ	YJW740	*top1-5FLAG:natMX6 rnh201::hphMX4*	This study

pol2-M644G top1-5FLAG rnh201Δ	YJW800	*pol2-M644G top1-5FLAG:natMX6 rnh201::hphMX4*	This study

Appendix Table S3 - Oligonucleotide sequences for the Top1 cleavage assay.

Name	Sequence (5'-3')
$(AG)_4$-NTS	AACGCTGAAG TGA***AGAGAGAGA G***CTTAAGCAA
$(AG)_4$-NTS-rU	AACGCTGAAG rUGA***AGAGAGAGA G***CTTAAGCAA
$(AG)_4$-TS	TTGCTTAAG***C TCTCTCT***TCA CTTCAGCGTT
$(AG)_4$-TS-5P	P-TTGCTTAAG***C TCTCTCT***TCA CTTCAGCGTT
$(AT)_2$-NTS	ACAAAGGTTT TGCCAC***ATAT*** CTTCAACGCT
$(AT)_2$-TS	AGCGTTGAAG ***ATAT***GTGGCA AAACCTTTGT
$(AT)_2$-TS-5-6R	AGCGrUrUGAAG ***ATAT***GTGGCA AAACCTTTGT
$(AT)_2$-TS-7-8R	AGCGTTrGrAAG ***ATAT***GTGGCA AAACCTTTGT
$(AT)_2$-TS-9-10R	AGCGTTGArArG ***ATAT***GTGGCA AAACCTTTGT
$(AT)_2$-TS-11-12R	AGCGTTGAAG ***rArUAT***GTGGCA AAACCTTTGT
$(AT)_2$-TS-13-14R	AGCGTTGAAG ***ATrArU***GTGGCA AAACCTTTGT
$(AT)_2$-TS-15-16R	AGCGTTGAAG ***ATAT***rGrUGGCA AAACCTTTGT
$(AT)_2$-TS-17-18R	AGCGTTGAAG ***ATAT***GTrGrGCA AAACCTTTGT
$(AT)_2$-TS-19-20R	AGCGTTGAAG ***ATAT***GTGGrCrA AAACCTTTGT
$(AT)_2$-TS-One-ribo	AGCGTTGAAG ***ArUAT***GTGGCA AAACCTTTGT
$(AT)_2$-TS-Two-ribo	AGCGTTGAAG ***rArUAT***GTGGCA AAACCTTTGT
$(AT)_2$-TS-Three-ribo	AGCGTTGAArG ***rArUAT***GTGGCA AAACCTTTGT
$(AT)_2$-TS-All-ribo	rArGrCrGrUrUrGrArArG ***rArUrArUr***GrUrGrGrCrA rArArArCrCrUrUrUrGrU

* Bold, italic fonts denote the positions $(AG)_4$ or $(AT)_2$ sequences. Ribonucleotides are in red.

TS: transcribed strand, NTS: non-transcribed strand.

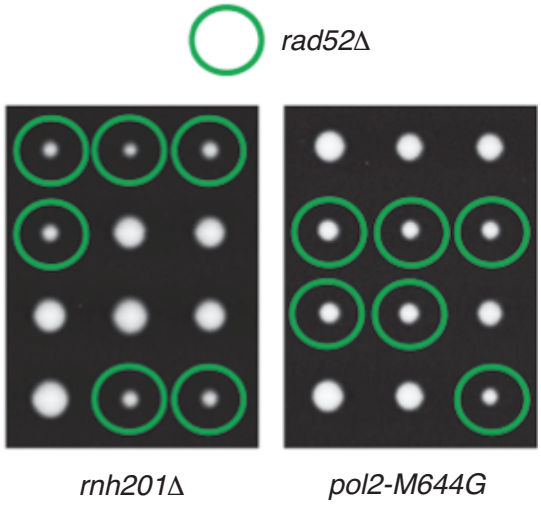

Appendix Figure S1 - *RAD52* is not essential for maintaining viability in the *rnh201Δ* or *pol2-M644G* control strains. *RAD52*/*rad52Δ* diploid dissections demonstrate that *RAD52* is dispensable for viability in an *RNase H2*-deficient strain containing wild type replicative polymerases (*rnh201Δ*) or in a strain containing *pol2-M644G* mutator allele yet is proficient in RNase H2 activity (*RNH201-WT*). Each column is a tetrad dissection. Plates were photographed after growth period of 3 days at 30 °C on rich medium.

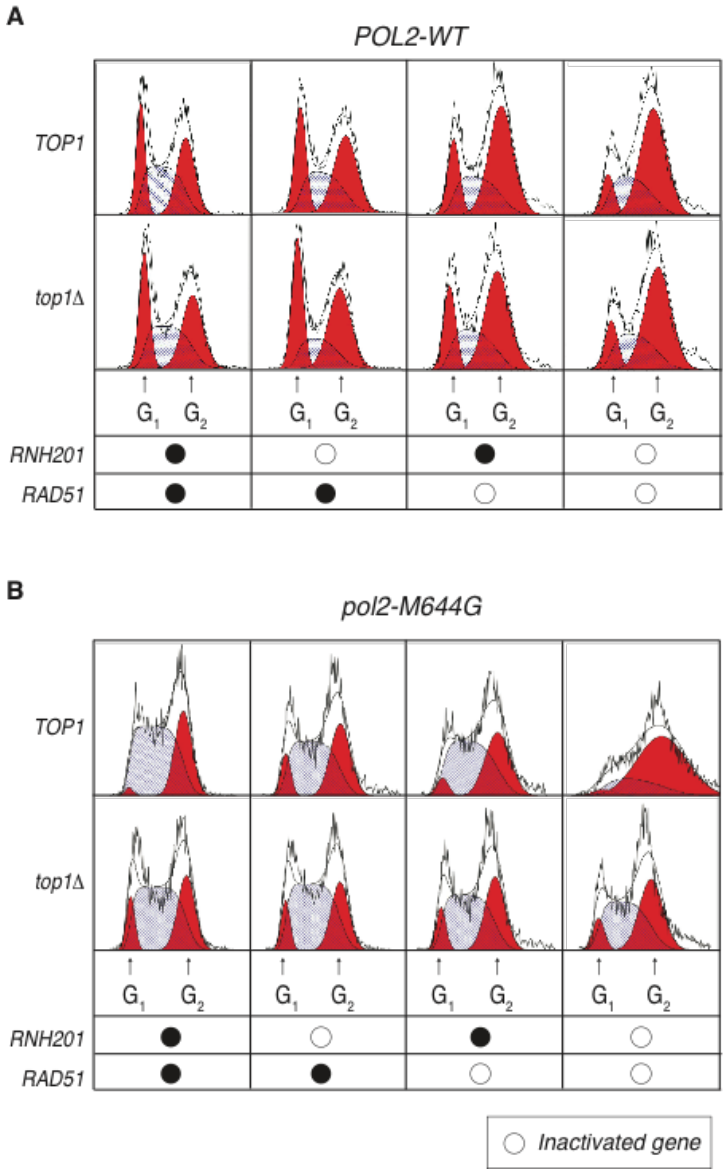

Appendix Figure S2 - Histograms displaying the disruption in cell cycle distribution caused by Top1-dependent genome instability in the *RNase H2* and/or *Rad51*-deficient yeast strains.

A *POL2-WT*.

B *pol2-M644G* (quantification is shown as bar graph in Fig 3B).

Open circles indicate inactivated genes for each strain. In each histogram, the horizontal axis represents the fluorescence parameter and the vertical axis represents the number of cells. The raw data (plotted lines) were fitted to cell cycle phase populations (smoothed lines) using ModFit software analysis. The red shaded areas represent cells in G_1 or G_2/M phases, the striped area represent cells in S phase.

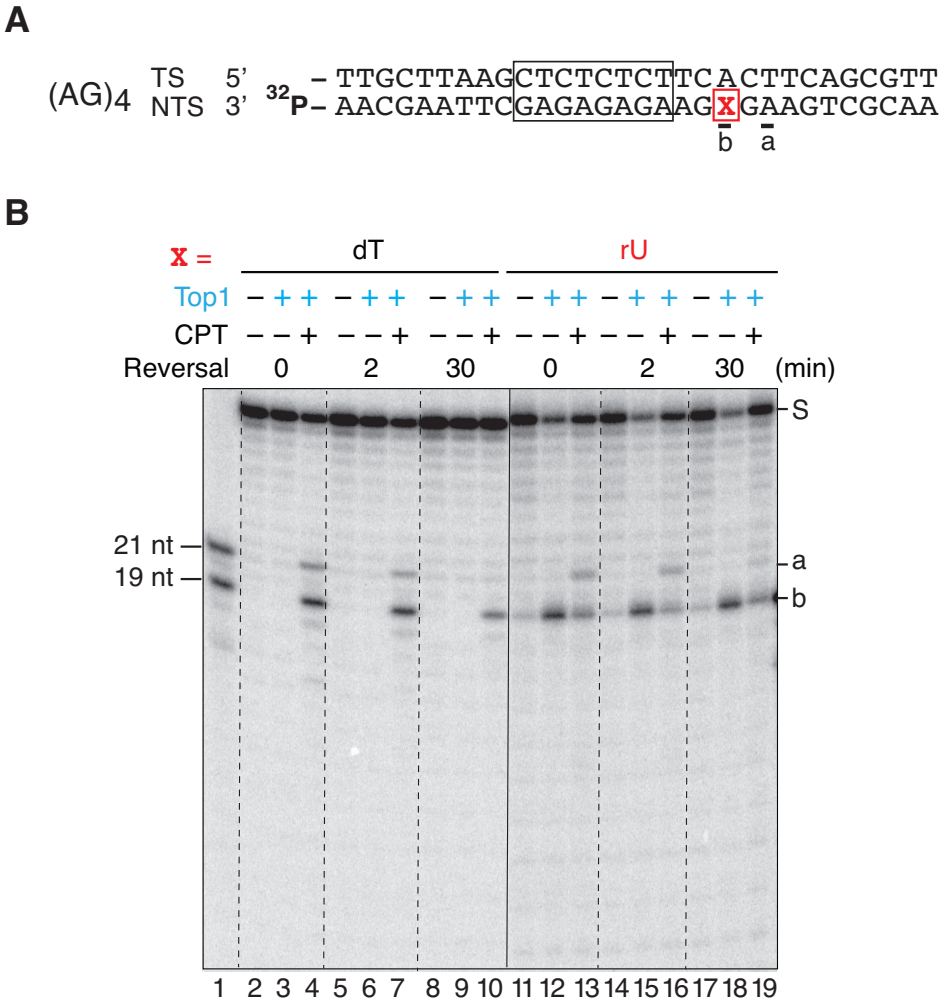

Appendix Figure S3 - Ribonuclease activity of Top1 induces irreversible nicks at ribonucleotide sites.

A DNA constructs containing the sequence from the *CAN1* $(AG)_4$ site (marked by a box) with the non-transcribed strand (NTS) radio-labeled at the 3'-end. Position X in the (NTS) contained either a deoxythymidine (dT) or a ribouridine (rU).

B Top1 cleavage and reversal assay with the DNA construct shown in panel A. Top1 cleavage reaction samples were allowed to reach equilibrium before addition of 0.5 M NaCl (final concentration) to reverse Top1 cleavage complexes. A small volume was withdrawn from the sample at the indicated time points and analyzed on a sequencing gel. Top1-induced products are labeled a-b. DNA markers of predicted sizes are loaded in lane 1. In the presence of a deoxyribonucleotide at the position X in the NTS, Top1 induced both cleavage sites only in the presence of camptothecin (CPT) (lane 4). Nevertheless, both Top1 cleavage products diminished with increasing time of reversal reaction (lanes 4, 7 and 10). In the case of a ribonucleotide at the position X, Top1 cleavage product at site a was CPT-dependent and reversible (lanes 13, 16, and 19). However, Top1 cleavage product at site b, which corresponded to the product of Top1 ribonuclease activity, was CPT-independent and irreversible (lanes 12, 15 and 18).

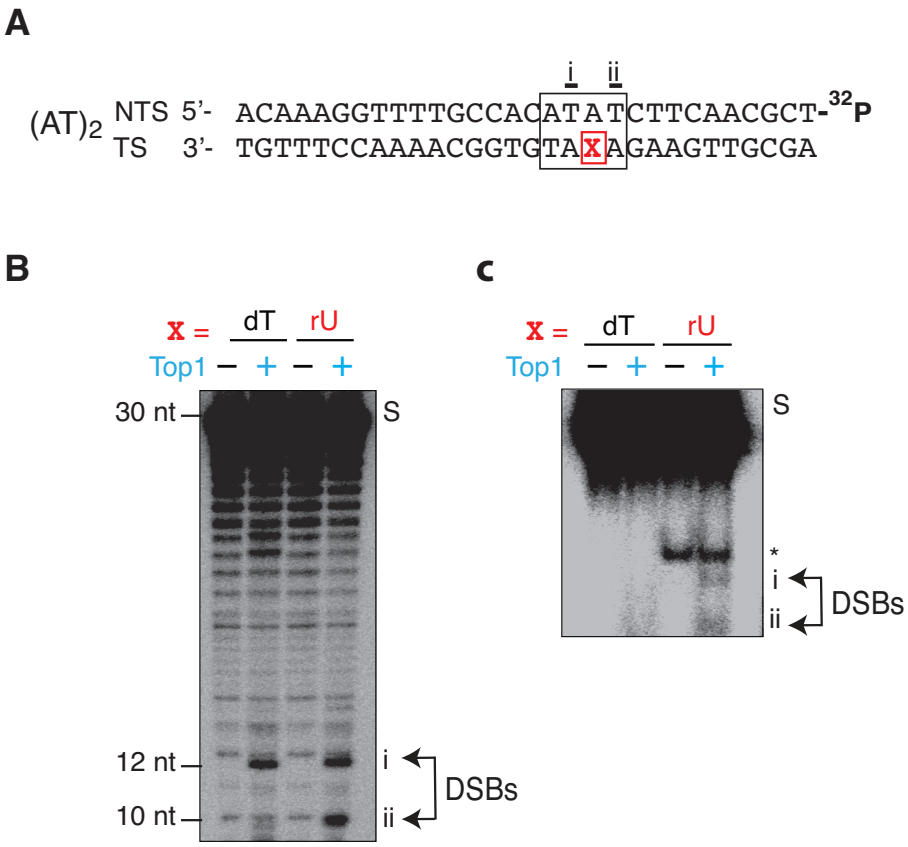

Appendix Figure S4 - Top1 induces DSBs in close proximity to ribonucleotide sites.

A DNA constructs containing the sequence from the *CAN1* $(AT)_2$ site (marked by a box) with the non-transcribed strand (NTS) radio-labeled at the 3'-end. Position X in the transcribed strand (TS) contained either a deoxythymidine (dT) or a ribouridine (rU).

B Representative gel image of Top1 cleavage assay with the construct shown in panel A, resolved on a denaturing sequencing gel. Top1-induced products are labeled i-ii, with the corresponding Top1 cleavage site labeled below the sequence in panel A.

C Top1 cleavage assay with the same construct resolved on a native gel. A non-specific product that is likely due to a partial melting of the nicked substrate is denoted by the asterisk.

Appendix References

Clark AB, Lujan SA, Kissling GE, Kunkel TA (2011) Mismatch repair-independent tandem repeat sequence instability resulting from ribonucleotide incorporation by DNA polymerase epsilon. DNA Repair (Amst) 10: 476-82

Endo K, Tago Y, Daigaku Y, Yamamoto K (2007) Error-free RAD52 pathway and error-prone REV3 pathway determines spontaneous mutagenesis in Saccharomyces cerevisiae. Genes & genetic systems 82: 35-42

Huang ME, Rio AG, Galibert MD, Galibert F (2002) Pol32, a subunit of Saccharomyces cerevisiae DNA polymerase delta, suppresses genomic deletions and is involved in the mutagenic bypass pathway. Genetics 160: 1409-22

Kim N, Huang S-yN, Williams JS, Li YC, Clark AB, Cho J-E, Kunkel TA, Pommier Y, Jinks-Robertson S (2011) Mutagenic processing of ribonucleotides in DNA by yeast topoisomerase I. Science 332: 1561-4

Kunz BA, Peters MG, Kohalmi SE, Armstrong JD, Glattke M, Badiani K (1989) Disruption of the RAD52 gene alters the spectrum of spontaneous SUP4-o mutations in Saccharomyces cerevisiae. Genetics 122: 535-42

Kunz BA, Ramachandran K, Vonarx EJ (1998) DNA sequence analysis of spontaneous mutagenesis in Saccharomyces cerevisiae. Genetics 148: 1491-505

Nick McElhinny SA, Kumar D, Clark AB, Watt DL, Watts BE, Lundström E-B, Johansson E, Chabes A, Kunkel TA (2010) Genome instability due to ribonucleotide incorporation into DNA. Nat Chem Biol 6: 774-81

Roche H, Gietz RD, Kunz BA (1995) Specificities of the Saccharomyces cerevisiae rad6, rad18, and rad52 mutators exhibit different degrees of dependence on the REV3 gene product, a putative nonessential DNA polymerase. Genetics 140: 443-56

Williams JS, Smith DJ, Marjavaara L, Lujan SA, Chabes A, Kunkel TA (2013) Topoisomerase 1-mediated removal of ribonucleotides from nascent leading-strand DNA. Mol Cell 49: 1010-5